De novo variants in SP9 cause a novel form of interneuronopathy characterized by intellectual disability, autism spectrum disorder, and epilepsy with variable expressivity

Marine Tessarech, Gaëlle Friocourt, Florent Marguet, Maryline Lecointre, Morgane Le Mao, Rodrigo Muñoz Díaz, Cyril Mignot, Boris Keren, Bénédicte Héron, Charlotte de Bie, et al.

▶ **To cite this version:**

Marine Tessarech, Gaëlle Friocourt, Florent Marguet, Maryline Lecointre, Morgane Le Mao, et al.. De novo variants in SP9 cause a novel form of interneuronopathy characterized by intellectual disability, autism spectrum disorder, and epilepsy with variable expressivity. Genetics in Medicine, 2024, 26 (5), pp.101087. 10.1016/j.gim.2024.101087 . hal-04530295

HAL Id: hal-04530295
https://hal.science/hal-04530295

Submitted on 3 Apr 2024

HAL is a multi-disciplinary open access archive for the deposit and dissemination of scientific research documents, whether they are published or not. The documents may come from teaching and research institutions in France or abroad, or from public or private research centers.

L'archive ouverte pluridisciplinaire **HAL**, est destinée au dépôt et à la diffusion de documents scientifiques de niveau recherche, publiés ou non, émanant des établissements d'enseignement et de recherche français ou étrangers, des laboratoires publics ou privés.

Distributed under a Creative Commons Attribution 4.0 International License

Genetics in Medicine (2024) 26, 101087

ELSEVIER

Genetics in Medicine
An Official Journal of the ACMG

www.journals.elsevier.com/genetics-in-medicine

ARTICLE

De novo variants in *SP9* cause a novel form of interneuronopathy characterized by intellectual disability, autism spectrum disorder, and epilepsy with variable expressivity

Marine Tessarech[1,2,*], Gaëlle Friocourt[3], Florent Marguet[4], Maryline Lecointre[4], Morgane Le Mao[2], Rodrigo Muñoz Díaz[2], Cyril Mignot[5], Boris Keren[5,6], Bénédicte Héron[7,8], Charlotte De Bie[9], Koen Van Gassen[9], Didier Loisel[10], Benoit Delorme[10], Steffen Syrbe[11], Annick Klabunde-Cherwon[11], Rami Abou Jamra[12], Meret Wegler[12], Bert Callewaert[13], Annelies Dheedene[13], Merzouka Zidane-Marinnes[14], Agnès Guichet[1,2], Céline Bris[1,2], Patrick Van Bogaert[15], Florence Biquard[16], Guy Lenaers[2], Pascale Marcorelles[17], Claude Ferec[3], Bruno Gonzalez[4], Vincent Procaccio[1,2], Antonio Vitobello[18,19], Dominique Bonneau[1,2], Annie Laquerriere[4], Salim Khiati[2], Estelle Colin[1,2,*]

ARTICLE INFO

Article history:
Received 12 May 2023
Received in revised form
22 January 2024
Accepted 23 January 2024
Available online 27 January 2024

Keywords:
Interneuronopathy
KLF/SP transcription factor
Neomorphic DNA-binding functions
Neurodevelopmental disorders
SP9

ABSTRACT

Purpose: Interneuronopathies are a group of neurodevelopmental disorders characterized by deficient migration and differentiation of gamma-aminobutyric acidergic interneurons resulting in a broad clinical spectrum, including autism spectrum disorders, early-onset epileptic encephalopathy, intellectual disability, and schizophrenic disorders. SP9 is a transcription factor belonging to the Krüppel-like factor and specificity protein family, the members of which harbor highly conserved DNA-binding domains. *SP9* plays a central role in interneuron development and tangential migration, but it has not yet been implicated in a human neurodevelopmental disorder.

Methods: Cases with *SP9* variants were collected through international data-sharing networks. To address the specific impact of *SP9* variants, in silico and in vitro assays were carried out.

Results: De novo heterozygous variants in *SP9* cause a novel form of interneuronopathy. *SP9* missense variants affecting the glutamate 378 amino acid result in severe epileptic encephalopathy because of hypomorphic and neomorphic DNA-binding effects, whereas *SP9* loss-of-function variants result in a milder phenotype with epilepsy, developmental delay, and autism spectrum disorder.

Conclusion: De novo heterozygous *SP9* variants are responsible for a neurodevelopmental disease. Interestingly, variants located in conserved DNA-binding domains of KLF/SP family transcription factors may lead to neomorphic DNA-binding functions resulting in a combination of loss- and gain-of-function effects.

Marine Tessarech, Gaëlle Friocourt, Salim Khiati, and Estelle Colin contributed equally.

*Correspondence and requests for materials should be addressed to Estelle Colin, CHU d'Angers, 4 rue, Larrey, Angers 49933, France. *Email address:* escolin@chu-angers.fr OR Marine Tessarech, CHU d'Angers, 4 rue, Larrey, Angers 49933, France. *Email address:* marine.tessarech@chu-lille.fr

Affiliations are at the end of the document.

doi: https://doi.org/10.1016/j.gim.2024.101087

1098-3600/© 2024 The Authors. Published by Elsevier Inc. on behalf of American College of Medical Genetics and Genomics. This is an open access article under the CC BY license (http://creativecommons.org/licenses/by/4.0/).

© 2024 The Authors. Published by Elsevier Inc. on behalf of American College of Medical Genetics and Genomics. This is an open access article under the CC BY license (http://creativecommons.org/licenses/by/4.0/).

Introduction

Central nervous system development is a highly complex process that spans from the fifth embryonic week to adulthood and takes place schematically in 2 phases. The first phase, referred to as anatomical construction, is associated with a high proliferative activity allowing the production of different neural cell populations from the germinative zones. Gamma-aminobutyric acidergic (GABAergic) interneurons are essential for establishing local circuits among the generated neuronal cell populations. GABAergic interneurons are divided into subgroups corresponding to functional differences according to their morphology, synaptic connections, and the expression of specific markers. In humans, GABAergic interneurons originate from progenitor cells located in the ventricular and subventricular zones of the basal telencephalon, including the median, lateral, and caudal ganglionic eminences (GEs), as well as the preoptic and preoptico-hypothalamic areas. The specification of GABAergic interneurons originating from GEs is linked to the expression of a set of regulatory genes encoding various transcription factors.[1,2] Then, interneurons migrate tangentially to reach their final destination and gradually acquire their characteristic morphology and molecular, biochemical, and synaptic properties. The emergence of morphological and functional diversity of interneurons is linked to the spatial and temporal specification of progenitor cells through additional specific transcription programs, either intrinsically encoded or activated by interactions with the local microenvironment. Any abnormality altering one or more of these steps may affect brain development or function, leading to interneuronopathies. This term was first coined in 2005 by Kato et al[3] in relation to X-linked lissencephaly with abnormal genitalia caused by mutations in *ARX*. Interneuronopathies have now been associated with many other neurodevelopmental disorders (NDDs) in humans, including lissencephalies, early-onset epileptic encephalopathies, autism spectrum disorder (ASD), and schizophrenic disorders,[4] with a considerable increase in identified causative genes because of advances in DNA sequencing techniques.

Members of the KLF/SP gene family, including *SP9*, play key roles in various biological processes, including stem cell maintenance, cell proliferation, embryonic development, tissue differentiation, and metabolism.[5] Their dysregulation has been implicated in several human disorders, particularly in cancers.[6] Proteins of the KLF/SP family are characterized by a highly conserved triple-C2H2 DNA-binding domain (DBD) located in the C terminus and comprising 3 tandem zinc fingers (ZFs) with conserved linker regions in between. Each C2H2-ZF domain interacts with 3 or more DNA bases, with specific residues binding preferentially to target sequences.[6-8]

SP9 has not yet been implicated in a specific human disease, but in mouse models, this transcription factor is critical for the proliferation, differentiation, and survival of striatopallidal projection neurons. Analyses of these models have also revealed a central transcriptional role of *sp9* in medial GE (MGE)–derived cortical interneuron development. They have demonstrated that its dysregulation alters the expression of other key transcription factors involved in interneuron migration, including *Arx*, *Lhx6*, *Lhx8*, *Nkx2-1*, and *Zeb2*.[9]

Our study provides in silico and in vitro evidence that de novo heterozygous variants in *SP9* cause a novel form of interneuronopathy with variable severity depending on the presence of loss- or gain-of-function variants.

Materials and Methods

Individuals and data sharing

Clinical information, laboratory findings, imaging, neuropathological data, and genetic testing for the 5 individuals reported here were collected and evaluated as part of standard clinical care. Genetic results were matched through Genematcher[10] and shared upon written informed consent obtained from all individuals or their parents.

The *SP9* variants described here were all identified using trio exome sequencing (ES) (details in Supplemental Data) and were deposited in ClinVar (accession numbers SCV001950995 - SCV001950998).[11] The ethics committee approved the study at Angers University Hospital (number 2021-148).

Autopsy procedures and neuropathological studies of individual 1

The fetal autopsy was performed following a standardized protocol[12] after obtaining the informed consent of both parents. Fetal biometric parameters were assessed according to Guihard-Costa et al.[13] Brain growth and macroscopic assessment of brain maturation, including gyration, were evaluated according to the criteria of Guihard-Costa et al[13] and using the atlas published by Feess-Higgins and Larroche.[14]

After fixation of the brain into a 10% formalin buffer solution for 2 months, several sections were obtained from all cortical areas, as well as from basal ganglia. Seven-micrometer sections obtained from paraffin-embedded

tissues were stained using hematoxylin-eosin. Immunohistochemical studies were carried out according to standardized protocols using antibodies listed in Supplemental Table 1. All immunolabelings were compared with a male control fetus aged 36 weeks of gestation (WG), whose brain was macroscopically and microscopically free of lesions.

Studies on cell lines

Plasmid construction

All SP9 mutants were generated using standard procedures from the Myc-DDK-tagged-Human SP9 plasmid (Origene, RC227808) using the CloneAmp HiFi PCR premix (Takara Bio, catalog no. 639298), Cloning Enhancer (Takara Bio, catalog no. 639615), and In-Fusion HD Cloning Plus Kits (Takara Bio, catalog no. 638910) according to the manufacturer's instructions and using primers listed in Supplemental Table 2. To assess SP9 subcellular localization, SP9 wild type (WT) and mutants were cloned in fusion with eGFP at the EcoR1 and ApaI restriction sites of the pEGFP-N1 vector (Addgene, #6085-1). In parallel, SP9 WT and mutants were generated without Myc or GFP using new primers (Supplemental Table 2). All generated plasmids were verified by enzyme digestion and Sanger sequencing.

Live-cell confocal imaging

T98G human glioblastoma cells were seeded at a density of 20,000 cells/well in 4 well glass bottom µ-slides (80427, Ibidi). Twenty-four hours later, they were transfected with 1 µg of plasmid (SP9 WT and mutants in fusion with eGFP) and 2 µL of lipofectamine 3000 (ThermoFisher, L3000008). All images were captured 24 hours after transfection using a Leica TCS SP8 confocal microscope with a 40X/1.20 water objective lens (Leica Microsystems) equipped with a GaAsP Hybrid detector (HyD), at 37 °C.

Luciferase assays

DNA fragments corresponding to ultra-conserved (uc) genomic elements and putative enhancer regions of the Arx gene (sequences are provided in Supplemental Information of the 5 Individuals; Supplemental Figure 5) were amplified by polymerase chain reaction from mouse genomic DNA (primers in Supplemental Table 2) and subsequently cloned into the pGL4.23 firefly luciferase vector (Promega, E8411) using the In-Fusion cloning strategy (Clontech).

N2a cells were transfected using lipofectamine 2000, 24 hours after plating 120,000 cells/well in 24-well plates (Starlab) with 500 ng of putative Arx regulatory regions cloned into the luciferase reporter plasmid pGL4.23 and 200 ng of Sp9-expressing vector (EGFP-Sp9) or the vector alone (pEGFP-N1, Addgene, #6085-1). In addition, to account for variations in transfection efficiency and cell number, cells were also co-transfected with 100 ng of pGL4.74 vector expressing the Renilla luciferase driven by the HSV thymidine kinase promoter (Promega, E6921). Forty-eight hours after transfection, cell lysis and firefly and Renilla luciferase activity measurements were performed on a Varioskan LUX multimode microplate reader (Thermo Scientific) using the Dual-Luciferase Reporter Assay System (Promega, E1910) according to the manufacturer's instructions. Transfections were performed in triplicate. The firefly luciferase activity was normalized according to the corresponding Renilla luciferase activity to correct transfection efficiency, and luciferase activity was reported as a mean relative to the results obtained with the EGFP-N1 expression vector alone. Each transfection was performed in triplicate and the experiment was conducted at least 3 times. Significant differences were assessed by one-way analysis of variance with Dunnett's post hoc statistical test using Prism software from GraphPad.

Bioinformatics analyses

All figures were generated using R (code available upon request). Variations in *SP9* transcript levels in the human brain among different developmental stages and anatomical regions were investigated using RNA sequencing (RNA-seq) and RNA microarray data from the Brain-Span Atlas of the Developing Human Brain.[15] This data set covers 16 brain regions, including 11 neocortical areas, and spans developmental periods from the 8th postconceptional week to the 40th postnatal year. Gene-level RPKM expression values were transformed to log2 (RPKM+1) values. To explore the temporal expression pattern of *SP9* in the cortex, samples from the same developmental time point were grouped together, and expression values across these samples were averaged as previously described.[16] The table with all the missense variants in *SP9* was exported from the gnomAD database (v2.1.1)[17] in a CSV file to compare the location of individuals' missense variants with control missense variants. The location of the domains was defined using data from Uniprot, and *P* values were obtained with a χ^2 test comparing proportions using MedCalc Software online. Evolutionary conservation of the SP9 domain sequences was determined with Clustal Omega using fasta sequences retrieved from the Uniprot database. The presence of variants in the *SP9* coding sequence in the healthy human population was searched for using the gnomAD database (v2.1.1). The effects of missense variants on protein structure and function were predicted using diverse in silico pathogenicity scores.[18]

Results

Germline *SP9* de novo variants are responsible for neurodevelopmental disorders

Individual 1 is a male fetus. His mother, a 29-year-old para 1, gravida 0 woman with no significant medical history, was referred to our prenatal diagnosis center at 32 WG after fetal brain ultrasonography (US), which revealed 2 cysts within

the choroid plexuses and moderate ventricular dilatation (Figure 1A and B). Magnetic resonance imaging (MRI), performed at 33 WG, confirmed moderate ventricular dilatation (12 mm) and 2 periventricular cystic lesions close to the frontal horns of the lateral ventricles, along with hyperintense and hypointense signals at periventricular areas on T1- and T2-weighted images, respectively. A second MRI performed at 34 WG showed bilateral and symmetric hypointensities in the GEs and caudate nuclei on T2-weighted images, which were isointense on T1-weighted images and showed a restricted apparent diffusion coefficient on diffusion tensor imaging (Figure 1C-F). More clinical details are given in the Supplemental Information of the 5 Individuals. Given the severity of brain abnormalities, the parents opted for a medical termination of pregnancy at 35 WG in accordance with French law.

Chromosomal microarray and viral analyses performed on amniocytes were normal, as well as the dosage of interferon alfa in the fetal blood, excluding interferonopathy. Subsequent trio ES allowed the identification of a heterozygous de novo variant in *SP9* (NC_000002.12:g.174337218A>C NM_001145250.2:c.1133A>C p.(Glu378Ala)), with no other variant in known disease-causing genes. *SP9* has one protein-coding transcript, ENST00000394967.3 NM_001145250.2 (MANE Select transcript) (Uniprot P0CG40), expressed in different areas of the human brain with its highest expression levels in the basal ganglia (Supplemental Figure 1). The variant identified was absent from the gnomAD database and was predicted to be disease-causing by 11 in silico algorithms. Furthermore, *SP9* is predicted to be intolerant to missense or protein-truncating variants with a pLi at 0.94 and a positive *z*-score (2.26). Hence, we concluded that the *SP9* variant identified in individual 1 was a disease-causing variant.

Through Genematcher,[10] we identified 4 additional individuals from 4 unrelated families harboring de novo heterozygous variants in *SP9*. Individuals 2, 3, 4, and 5 ranged in age from 6 months to 6 years (median: 3.5 years), and all had an NDD of variable severity. Their clinical features are summarized in Table 1 and in Supplemental Information of the 5 Individuals.

A first clinical phenotype consisting of moderate intellectual disability (ID) associated with an ASD with or without epilepsy was present in individuals 2 and 5 who carried frameshift *SP9* variants, p.(His406Thrfs*2) and p.(Arg403Glnfs*15), respectively. A second, more severe clinical phenotype consisting of epileptic encephalopathy was present in individuals 3 and 4, who both carried a missense variant p.(Glu378Gly) involving the same glutamate residue in position 378 as individual 1.

SP9 is expressed in regions crucial for the development of cortical interneurons

To better understand the role of *SP9* in the brain, we performed bioinformatics analyses using available RNA-seq data from the developing human brain.[15,19] By examining *SP9* expression at several developmental time points, we found that *SP9* expression was the highest before post-conceptional week 24 (Figure 2A), followed by a decreased expression in the cortex. This suggests that *SP9* is more critical during the first half of gestation. We next examined single-cell transcriptomic data from the developing human brain.[20] They revealed that *SP9* is expressed in the developing interneurons of the caudal GE and MGE (Figure 2B). Finally, by studying the spatiotemporal expression of *SP9*, we observed that this gene is first expressed in the GEs, then in the amygdala and striatum, and finally in the cortical plate, thus following the pattern of tangential migration of GABAergic interneurons (Figure 2C).[2,19]

Neuropathological assessment of the fetal brain of individual 1 shows a significant depletion of MGE-GABAergic–derived interneurons

The frontal lobes appeared slightly hypoplastic on macroscopic examination, and the sylvian fissure was prematurely closed (Figure 3A), but no other gyral abnormalities were observed. On coronal sections, the most intriguing feature was the presence of several "heterotopic" nodules (Figure 3B) arising from voluminous GEs surrounding hypoplastic basal ganglia (Figure 3D) compared with the control (Figure 3C) and protruding into the ventricular cavities (Figure 3F) corresponding to the thickening of the ventricular wall observed on MRI (see Figure 1). Histological analysis displayed a 6-layered cortical plate. Still, layer IV appeared abnormally thick because of severe interneuron depletion in layer III, which contained almost exclusively pyramidal neurons (Figure 3G and H). Also, the ventricular and subventricular zones of the dorsal telencephalon, which normally disappear from 24 WG, abnormally persisted in individual 1 (Figure 3E).

A neuropathological assessment of the fetal brain of individual 1 revealed a defect in GABAergic interneuron production (Supplemental Figures 2, 3, and 4). Indeed, immunohistochemical studies using markers of GABAergic neurons (ARX, somatostatin, and calretinin) revealed a defect in the production of these neurons in the cerebral cortex of individual 1 (Supplemental Figure 2). Similarly, a severe depletion in ARX-, somatostatin-, calbindin-, and parvalbumin-positive interneurons was identified in the putamen and pallidum of individual 1 (Supplemental Figure 3). Taken together, these results argue for a major depletion of the 3 major subclasses of MGE-derived interneurons.

PTVs causing a *SP9* loss-of-function result in a clinical phenotype including ID, epilepsy, and ASD

The frameshift variants p.(His406Thrfs*2) and p.(Arg403Glnfs*15) are predicted in silico to be disease-causing because *SP9* is intolerant to loss-of-function

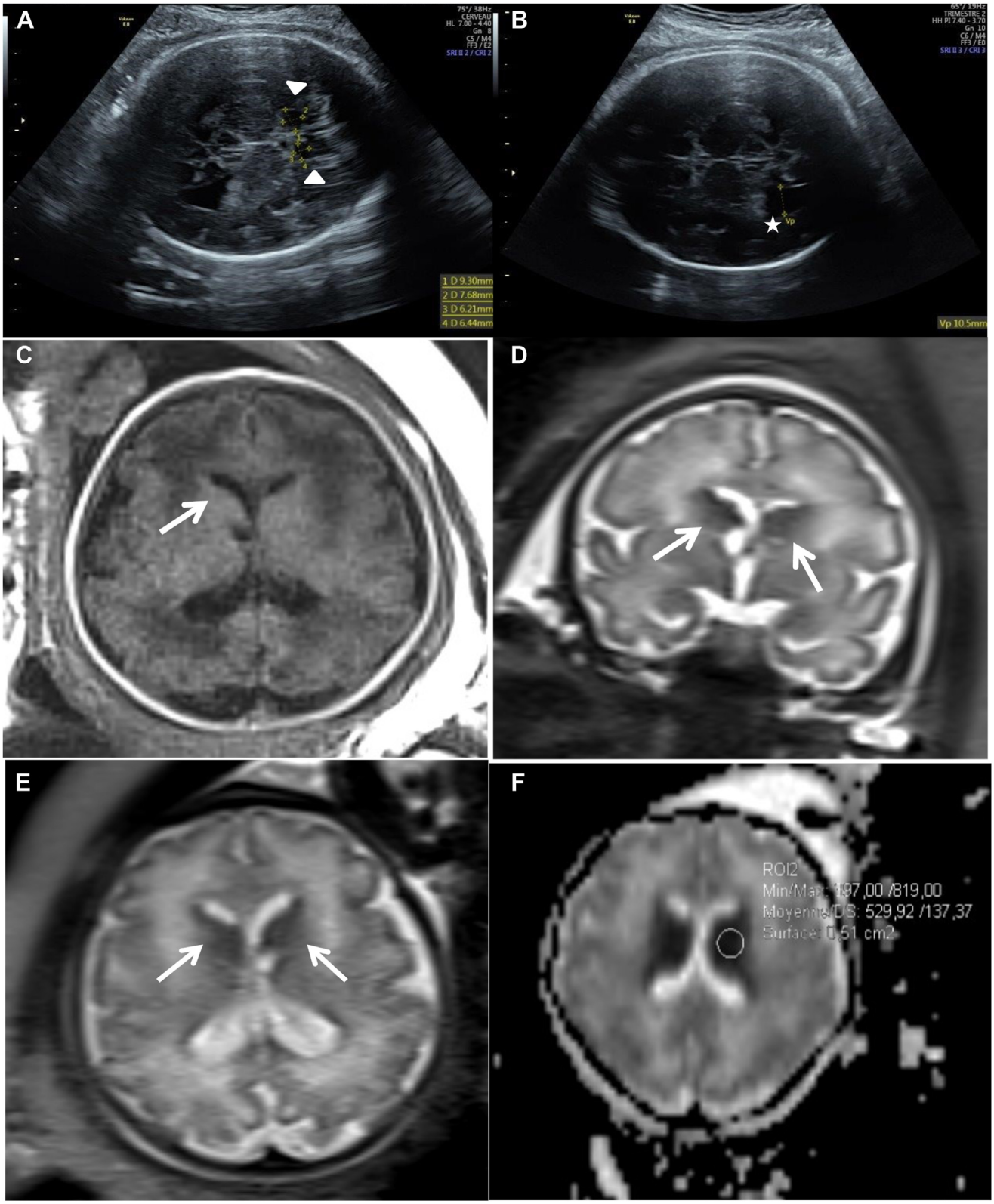

Figure 1 Fetal brain imaging of individual 1 showing abnormalities in the ganglionic eminences and caudate nuclei. A and B. Ultrasound images obtained at 32 weeks of gestation (WG) show 2 cysts in the choroid plexuses (white arrows) and ventricular dilatation (white star). C-E. Magnetic resonance images obtained at 34 WG confirm the ventricular dilatation (12 mm) and the bilateral periventricular cystic lesions close to lateral ventricles and show symmetric hypointensities (white arrows) in the ganglionic eminences and caudate nuclei on T2-weighted images (D and E), which are isointense on T1-weighted images (C). F. Diffusion tensor imaging showing a restricted apparent diffusion coefficient.

Table 1 Clinical features of individuals with missense and truncating variants in *SP9*

	Individual 1	Individual 2	Individual 3	Individual 4	Individual 5
Variant in *SP9* (NM_001145250.1)	NC_000002.12:g.174337218A>C NM_001145250.2:c.1133A>C p.(Glu378Ala)	NC_000002.12:g.174337301del NM_001145250.2:c.1216del p.(His406ThrfsTer2)	NC_000002.12:g.174337218A>G NM_001145250.2:c.1133A>G p.(Glu378Gly)	NC_000002.12:g.174337218A>G NM_001145250.2:c.1133A>G p.(Glu378Gly)	NC_000002.12:g.174337277_174337292dup NM_001145250.2:c.1192_1207dup p.(Arg403GlnfsTer15)
Exon (/2)	2	2	2	2	2
Variant ACMG classification	Likely pathogenic (class 4) PM2_supporting (absent from controls), PM6 (de novo, with a phenotype compatible with the gene but not highly specific) PM1 (located in a mutational hotspot without benign variations), PS3 (in vitro functional studies supportive of a damaging effect on the gene or geneproduct)	Likely pathogenic (class 4) PM2_supporting (absent from controls), PM6 (de novo, with a phenotype compatible with the gene but not highly specific) PM1 (located in a mutational hotspot without benign variations), PS3 (in vitro functional studies supportive of a damaging effect on the gene or gene product)	Likely pathogenic (class 4) PM2_supporting (absent from controls), PM6 (de novo, with a phenotype compatible with the gene but not highly specific) PM1 (located in a mutational hotspot without benign variations), PS3 (in vitro functional studies supportive of a damaging effect on the gene or gene product)	Likely pathogenic (class 4) PM2_supporting (absent from controls), PM6 (de novo, with a phenotype compatible with the gene but not highly specific) PM1 (located in a mutational hotspot without benign variations), PS3 (in vitro functional studies supportive of a damaging effect on the gene or gene product)	Likely pathogenic (class 4) PM2_supporting (absent from controls), PM6 (de novo, with a phenotype compatible with the gene but not highly specific) PM1 (located in a mutational hotspot without benign variations), PS3 (in vitro functional studies supportive of a damaging effect on the gene or gene product)
Mode of inheritance	De novo	De novo	De novo	De novo	De novo
Gender	M	M	F	F	M
Age at last investigation	TOP at 36 WG	Almost 6 y	6 mo (age of death, cardiorespiratory arrest)	16 mo	5 y 8 mo
Gestational wk	36	40+6	38	41	38
Birth weight in g (percentile)	2969.6 (97th percentile)	3430 (50th percentile)	3280 (50th percentile)	3410 (50th percentile)	3110 (50th percentile)
Birth length in cm (SD)	49 (2 SD)	NA	51 (75th percentile)	52 (−0.0.9 SD)	49
Birth head circumference in cm (percentile)	31.5 (−1,75 SD)	NA	34 (50th percentile)	33 (25th-50th percentile)	38.5 at age 2 mo
Growth failure	No	No	No	No	No
Overgrowth	Yes	No	No	No	No
Weight at age last investigation (kg/ percentile)	2.969 (97th percentile)	18 kg (10th percentile)	7.3 (50th percentile)	11.6 (50th percentile)	17.9 (25th percentile)
Height at age last investigation (cm/SD)	49 (+2 SD)	112 (−1.4 SD)	67(+1 SD)	80 (+0.12 SD)	110.5 (−1 SD)
Head circumference at age last investigation (cm/SD)	31.5 (−1.75 SD)	48 (−2.2 SD)	41 (−2 SD)	43.5 (−3.41 SD)	49.3 (−2 SD)
Developmental delay or ID	NA	Yes	Yes	Yes	Yes
Age of walking (mo)	NA	24	NA	Not yet	15
Age of first words	NA	2.5 y	NA	No words	No comprehensible words
Speech abilities	NA	Sentences of 3-5 words at 6 y	NA	Not yet	Sounds, but can sing melodies
Hypotonia	NA	Axial hypotonia	Global hypotonia of trunk and limbs	Severe global hypotonia	No
Hypertonia	NA	No	Progressive pyramidal signs and dyskinesia	No	Hyperreflexia of the lower limbs
Seizures, age of first, type	NA	Yes, 7 mo infantile spasms that disappeared spontaneously and at 4 yr, tonic-clonic seizures and absences	Yes, 25 d of age, focal migrating seizures with onset of focal seizures (apnea, clonic and/or tonic seizures, facial flushing)	Yes, first day of life, up to 40 seizures per day with multifocal onset during first months, generalized-onset seizures, multifocal-onset clonic seizures, infantile spasms, therapy-refractory	No

(continued)

Table 1 Continued

	Individual 1	Individual 2	Individual 3	Individual 4	Individual 5
EEG anomalies	NA	Epileptiform activity alternately left or right temporal-occipital	Slow background without developmentally appropriate features. Multifocal spikes, and focal spike and wave discharges predominantly in temporal and occipital areas, with ictal rhythms migrating from one cerebral region to another	Pathogenic, multifocal spikes and seizure patterns	No
Brain imaging age	Yes 32+5 WG and 34 WG	Yes 4 y and 9 mo	Yes 1 mo and 6 mo	Yes 1 wk and at 2 mo	Yes 4 y 3 mo
Anomalies in brain imaging	Two choroid cysts; mild ventriculomegaly; abnormal caudate nuclei	No	At 1 mo of age: bilateral subependymal hemorrhages At 6 mo of age: dedifferentiation of almost the entire temporal lobe, the lower part of the parietal lobe, and the anterior part of the occipital lobe on the right, associated with hyperperfusion in the ASL sequence.	At 1 wk and 2 mo: normal	Peritrigonal punctiform T2 hyperintense signal alterations-likely delayed myelinization
Sleep disturbance	NA	Wakes up once every night	Very little waking	Mild	No
Behavioral anomalies	NA	Hyperactive, hand flapping	NA	No	Tempers
Hearing loss/problems	NA	No	No	No	No
Cardiac anomalies	No	Not investigated	No	None	No
Eye anomalies	No	No	Poor visual contact, no ocular pursuit	Epicanthus	Strabism left eye (amblyopia)
Urogenital/kidney anomalies	Absence of the median raphe of the scrotum	Not investigated	No	No	No
Hands (eg, syndactyly, brachydactyly)	No	Fetal finger pads	Hypoplasia of 1 fingernail	No	No
Feet (eg, syndactyly, brachydactyly)	Claw feet	Sandal gap	No	No	No
Thorax (eg, scoliosis)	No	No	No	No	No
Palate anomalies (eg, high palate, cleft)	No	High palate	No	No	No
Feeding difficulties	NA	Yes	Swallowing difficulties requiring enteral nutrition from 5.5 mo of age	No	No
Facial dysmorphism	Cupped ears, retrognathia, squared forehead	Mild upslant of the eyes, large eyes with long eye lashes, arched eyebrows, thin upper lip, small chin	No	Abnormal facial shape	High nasal bridge, midface hypoplasia, short midface, flat philtrum, thin upper lip, horizontal smile, slightly limited opening of the mouth, pointed chin, post rotated ears
Other anomalies or problems	No	Hypertrichosis upper arms and back, hypermobility	No	No	No

ACMG, American College of Medical Genetics and Genomics; *EEG*, electroencephalogram; *F*, female; *ID*, intellectual disability; *M*, male; *NA*, not available; *TOP*, termination of pregnancy; *WG*, weeks of gestation.

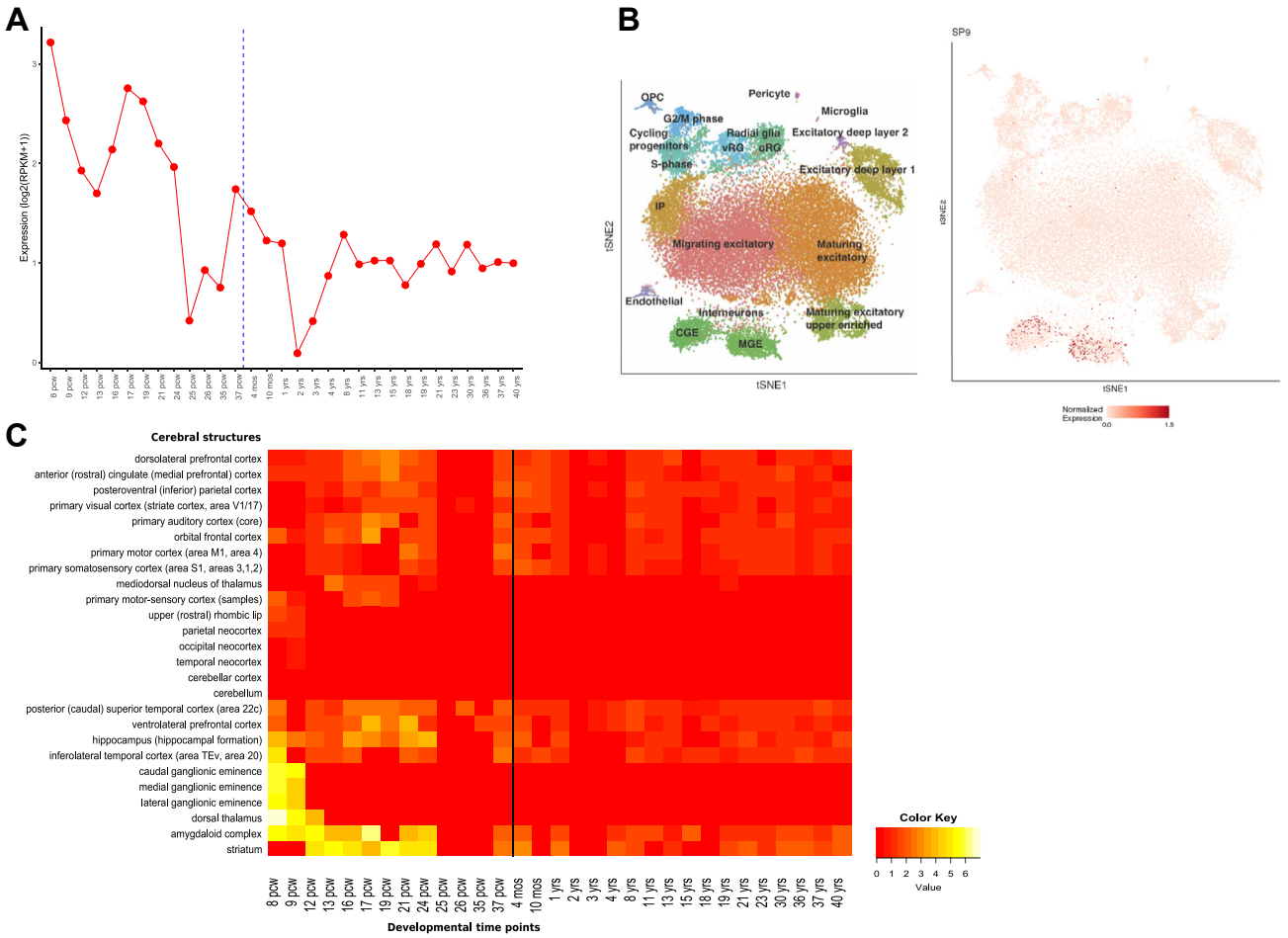

Figure 2 Temporospatial expression of *SP9* in the brain. A. Expression of *SP9* during neocortical development. The expression values of *SP9* across cortical samples are grouped and sorted by developmental time points. The dotted line corresponds to birth. B. Scatter plot visualization of cells of the developing human neocortex after t-stochastic neighbor embedding (tSNE), colored by cell-type annotation with the normalized expression level of *SP9*. C. Heatmap of *SP9* expression at different developmental time points and in different cerebral structures.

variants, as indicated by its pLi (0.94) and Loeuf (0 [0-0.34]) scores (gnomAD v2.1).[21] Both variants are located in the C2H2-type 3 ZF protein domain, which is required for DNA binding (Figure 4A and B).[5] In the gnomAD database, only 4 *SP9* nonsense variants are located downstream from the C2H2 ZF domains.

We first investigated whether the p.(His406Thrfs*2) variant could change SP9 subcellular localization. Therefore, we generated a GFP-tagged protein construct and assessed its localization using live-cell fluorescence confocal microscopy in the T98G cell line. As shown in Figure 4C, the p.(His406Thrfs*2) variant revealed a nuclear localization similar to that observed with WT-SP9-GFP.

Next, because Liu et al[9] have reported that in mice, Sp9 regulates the expression of several essential transcription factors for the development of cortical and striatal interneurons, in particular *Arx*, we experimentally tested *SP9* fixation on these regions and the effect of the variants identified in patients. Several putative enhancer regions (uc regions uc463 to uc469[22]) were identified upstream of the *Arx* coding sequence based on their high evolutionary conservation (Supplemental Figure 5A). They correspond approximately to the loci identified by Liu et al[9] using chromatin immunoprecipitation.[9] Furthermore, we showed that SP9 robustly activated the transcription of the luciferase gene when located downstream of the genomic regions uc462, 467, and 468 (Supplemental Figure 5B), suggesting that SP9 specifically binds to these regions and can activate transcription from these enhancer regions. However, the p.(His406*) variant affected the ability of SP9 to bind to these 3 enhancer regions and thus to activate the transcription of the reporter gene, confirming the expected mechanism of loss of function (Figure 4D).

Variants affecting recurrently the glutamate residue in position 378 in *SP9* DBD generate neomorphic and hypomorphic effects leading to epileptic encephalopathy

The C2H2 ZF domains are highly conserved in all KLF/SP family transcription factors and are required for proper DNA

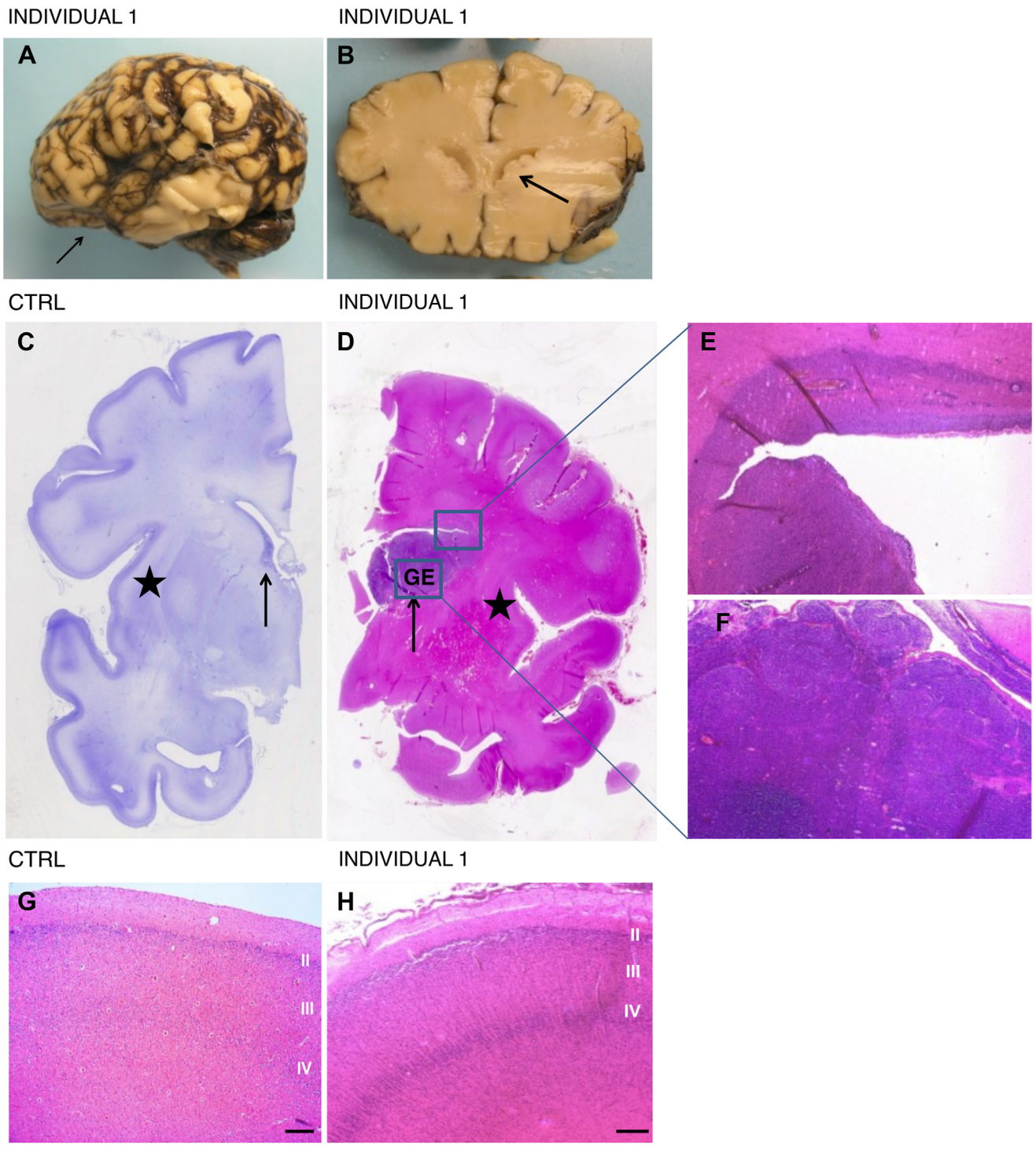

Figure 3 **In individual 1, the regions of the brain producing GABAergic neurons have an abnormal development.** A. Macroscopic view of the left hemisphere showing tertiary sulci but with premature closure of the Sylvian fissure (black arrow). B. On the coronal section through the striatum, multiple small nodules protrude into the anterior horns of the lateral ventricles (black arrow). C and D. On whole-mounted sections at the same magnification, the ganglionic eminences are voluminous and made of multiple nodules (black arrow) (D), and the caudate and lenticular nucleus are hypoplastic (D) compared with the control brain in which ganglionic eminences have almost completely regressed (black arrow) with normal morphology of the caudate and lenticular nucleus (black star) (C) ([C]: HE, [D]: Cresyl violet). E and F. Persistence of the germinative zone of the dorsal telencephalon (E) and lateral ganglionic eminence (F) (HE, original magnification X100). G and H. Histological analysis of the cortical plate showing an abnormally apparent layer IV because of the severe depletion of GABAergic neurons in layer III (HE, original magnification X 20). HE, hematoxylin staining; scale bars: 0.3 mm.

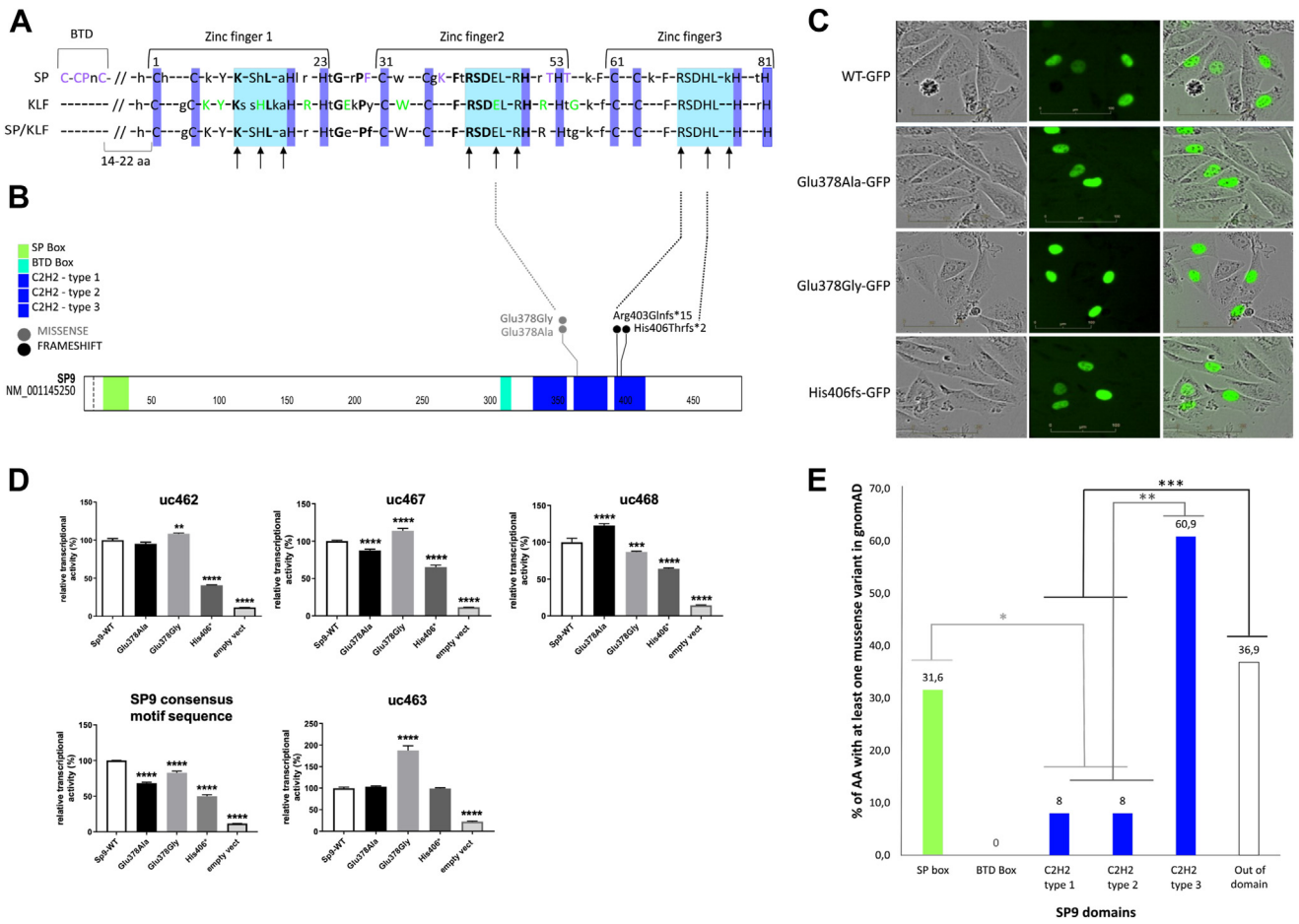

Figure 4 ***SP9* pathogenic variants are located in DNA binding sites of the protein.** A. Characteristic hallmarks of SP/KLF family members. Consensus sequences for the zinc-finger domains of all the SP and KLF transcription factors in human (25 transcription factors), *Drosophila* (9 transcription factors), and *C. elegans* (6 transcription factors) are shown for the SP transcription factors, the KLF transcription factors, and the entire family. All DNA-binding domains comprise 81 aa, with the exception of those of Ce-Y40B1A.4 (finger 1: CXXC instead of CXXXXC), Ce-T22C8.5 (finger 3: HXXXXH instead of HXXXH), and D-BTD (finger 2: CXXC instead of CXXXXC). The highly conserved BTD box located at the N terminus of the zinc fingers is a unique feature of the SP transcription factors. Bold capital letters indicate residues that are 100% conserved between all family members (black), between all KLF transcription factors (green), or between all SP transcription factors (purple). Capital letters indicate N90% conservation and lowercase letters N75% conservation. Blue bars indicate cysteine and histidine residues implicated in zinc coordination. Turquoise bars are supposed to be in contact with DNA. Arrows point to residues that probably determine C2H2 recognition by specific contacts with DNA bases. (Adapted from G Suske. Genomics 2005). B. Position of missense (in gray) and frameshift (in black) variants along *SP9* sequence. C. Fluorescence microscopy images of T98G cells transfected with the indicated *SP9* constructs. D. Effects of SP9 mutants on its binding to candidate regions uc462, uc463, uc467, and uc468 of *ARX* and subsequent activation of luciferase reporter gene transcription. Significant differences ($n = 3$) were assessed by one-way analysis of variance with Dunnett's post hoc statistical test: $^{**}P < .01$, $^{***}P < .001$, $^{****}P < .0001$. E. Percentage of amino acids per SP9 domain that feature at least 1 missense gnomAD variant. The P values obtained by χ^2 for the comparison of variant proportions between the different regions of *SP9* are shown.

binding.[6,7,23] Interestingly, all 3 *SP9* missense variants reported here involve the same glutamate at position 378, which is among the most conserved amino acids in the finger domain and is thought to contribute to base-specific recognition in the DNA target sequence[5] (Figure 4A and B). Furthermore, we compared the locations of patients' variants in *SP9* sequence with those of the gnomAD database, containing human population genetic variations. By performing χ^2 proportion comparisons, we found a statistically significant difference ($P < .005$) between the proportion of the population missense variants in C2H2-type 1 and 2 ZF domains versus other *SP9* domains (SP box and C2H2-type 3 ZF) and versus other regions located outside these domains (Figure 4E). This suggests that the C2H2-type 1 and 2 ZF domains are intolerant to missense variants and could be a missense variant hotspot. In contrast, many missense variants are present in gnomAD in the C2H2-type 3 ZF domain, suggesting it is more tolerant to missense variants (Figure 4E).

Next, using HOPE,[18] we predicted changes in amino acid properties that could disturb the ZF domains' DNA-binding function. The replacement of glutamate 378 by either an

alanine or a glycine induces similar changes regarding the amino acid's charge, size, and hydrophobicity. Both variants p.(Glu378Ala) and p.(Glu378Gly) result in a loss of negative charge and replace the glutamate with a smaller amino acid, which could result in a loss of interactions with DNA.

In addition, the 2 more hydrophobic residues located at position 378 can lead to the loss of hydrogen bonds and/or disrupt the proper folding of the protein. Finally, as glycine is a very flexible molecule, its presence at position 378 may disrupt the required rigidity of the protein.

We then confirmed that both missense variants do not alter the subcellular localization of SP9 (Figure 4C).

Interestingly, luciferase assays performed with the p.(Glu378Ala) and p.(Glu378Gly) missense mutants showed different capacities of transcription activation, depending on the uc region tested (Figure 4D), thus suggesting an alternative disease-causing mechanism.

To further investigate the effects of these mutations, we first tested a genomic sequence containing several SP9 consensus binding motifs (Supplemental Figure 5A). As shown in Figure 4D, the 3 mutants showed less affinity for this sequence than WT SP9, suggesting a loss-of-function effect of p.(Glu378Ala) and p.(Glu378Gly), similar to the p.(His406*) variant. However, when the binding of these mutants was tested on the uc463 region, a sequence on which WT SP9 does not bind (Supplemental Figure 5B), the Glu378Gly mutant exhibited high levels of unspecific binding to uc463 resulting in an expression of the reporter gene (Figure 4D). Similarly, the Glu378Ala mutant exhibits higher activation of the reporter gene at the uc468 genomic region than WT SP9, again suggesting stronger binding of the mutant protein at this location (Figure 4D). From all these results, we can conclude that variants affecting the glutamate residue in 378 of SP9 have an increased affinity for other binding sites than those usually targeted by WT SP9, resulting in neomorphic DNA-binding functions.

Discussion

This study describes a novel form of interneuronopathy caused by de novo heterozygous variants in *SP9*, which encodes a transcription factor mainly expressed during brain development, particularly in the basal ganglia. Bioinformatics analyses suggested that *SP9* is preferentially expressed during prenatal rather than postnatal brain development and has an expression pattern in the developing cerebral cortex and basal ganglia that follows the tangential migration of GABAergic interneurons, thus reinforcing the hypothesis that *SP9* is involved in interneuron development.

At the neuropathological level, the interneuronopathy observed in the brain of individual 1 is characterized by voluminous and dysmorphic GEs because of the accumulation of immature interneurons. A defect in both interneuron generation and tangential migration probably caused this accumulation. This is suggested by the absence of ARX expression in the GEs and by a severe neuronal depletion of cortical interneurons in cortical layer III. These abnormalities are identical to those observed during the development and migration of GE-derived interneurons in Sp9 null and conditional mutant mice[24]: a reduction in GE-derived cortical interneurons with ectopic aggregation of GE-derived neurons in the embryonic ventral telencephalon.[9] In addition, chromatin immunoprecipitation seq data obtained in the MGE[9] revealed that Sp9 binds to loci in the region of Arx and of other key transcription factors involved in interneuron development, including *Lhx6*, *Lhx8*, and *Zeb2*. Consistently, these genes have a significantly reduced expression, as shown on RNA-seq data obtained in the MGE of *Sp9* mouse models. Therefore, this conditional knockout mouse could be used as a comparison model. Indeed, neomorphic missense variants' functional outcomes can be considered as the result of the loss-of-function effect represented by reduced endogenous SP9 occupancy and the gain-of-function effect defined by increased occupancy at endogenous and new SP9 loci.[25]

Moreover, expression profiles of several transcription factors involved in rodent GEs are also found in primates,[26,27] and transcriptional profiles of genes controlling the specification, migration, and differentiation of GABAergic neurons are conserved throughout evolution.[26] Data obtained from animal models and our results strongly suggest that *SP9* plays a critical role in the development of GABAergic interneurons necessary for neocortical functioning.[9,24,28-31]

Kawakami et al[32] found that *Sp9* and *Sp8* play a role in proper limb outgrowth in chick, mouse, and zebrafish models. However, no limb defects were noted in our series, suggesting that *SP9* may not be involved in limb development in humans.

We observed here 2 main types of NDDs, distinguished based on their molecular mechanism. *SP9* loss-of-function variants in the third C2H2-binding domain cause ID, ASD, and epilepsy, whereas missense variants in the second C2H2-binding domain result in hypomorphic and neomorphic DNA-binding functions that cause severe epileptic encephalopathy. Depending on the variation type and position, this broad spectrum of disorders has previously been reported, for example, with *ARX*, another transcription factor involved in GABAergic interneuron development.[33] We showed that the frameshift variant p.(His406Thrfs*2) reduces SP9 binding to putative *ARX* regulatory sequences to which SP9 typically binds. The p.(Arg403Glnfs*15) variant is located in the same C2H2-type 3 ZF domain, a very conserved residues. Indeed, both variants, NM_001145250.1: c.1216del (p.(His 406Thrfs*2)) and NM_001145250.1: c.1192_1207dup (p.(Arg403Glnfs*15)) are found in exon 2/2. Therefore, we strongly think that this variant will show very similar results to the ones that we obtained with the p.(His406Thrfs*2) variant. This loss of function could be explained by a nonsense-mediated decay. Indeed, if the frameshift variants lead to nonsense-mediated decay, the unaffected allele can still be expressed, but the amount of protein is reduced, which cannot

compensate for the loss of function of the mutant allele. A stable truncated messenger RNA with a truncated mutant protein. Variants that occur in the final exon evade degradation and are translated normally. However, the resulting truncated proteins do not have the properties of the WT protein. The second hypothesis most certainly explains the loss of function of our variants. In contrast, missense variants affecting the glutamate residue at position 378 involve a more complex pathogenic mechanism. This glutamate controls the recognition specificity of ZF through specific contacts with DNA bases.[5] Using in vitro models, we provide evidence that both variants p.(Glu378Ala) and p.(Glu378Gly) alter SP9 DNA-binding specificity by reducing binding to its usual targets and providing stronger binding to nonspecific regions. Ilsley et al[34] recently described a similar molecular mechanism for *KLF1*, a gene also belonging to the same KLF/SP family of transcription factors. The variant p.(Glu325Lys) in *KLF1* has been recurrently involved in congenital dyserythropoietic anemia type IV, a rare and severe autosomal dominant disorder. Ilsley et al[34] reproduced the deleterious effect of this variant on murine erythroid cell lines and demonstrated that it altered the DNA-binding specificity of KLF1, generating aberrant DNA binding. Interestingly, the glutamate 325 located in the second C2H2 ZF domain of KLF1 corresponds exactly to glutamate 378 of SP9 (Supplemental Figure 6). These glutamates constitute a unique and crucial specific DNA-binding site in these 2 proteins and all KLF/SP family proteins because they are highly conserved in this family of transcription factors. Ilsley et al[34] showed that neomorphic mutation at p.Glu325 in KLF1 causes altered broad genomic occupancy. However, wild-type and mutated (neomorphic) KLF1 proteins also showed shared regions with comparable occupancy levels. The same mechanism may take place in *SP9* neomorphic and hypomorphic variants.[25]

In conclusion, we have identified a novel type of interneuronopathy caused by de novo heterozygous variants of *SP9* and characterized by a broad spectrum of NDDs. Our results are consistent with those previously reported in conditional knockout Sp9 mouse models and provide additional insights into the pathogenesis of interneuronopathies. We also confirm that variants in highly conserved residues of the DBD of KLF/SP family transcription factors lead to neomorphic DNA-binding functions. However, the study of a larger number of individuals carrying pathogenic variants of *SP9* is required to expand the clinical phenotypic spectrum of this condition. Similarly, further functional studies are needed to confirm transcriptional defects for other loss-of-function and neomorphic variants of *SP9*, which may open new therapeutic avenues.

Data Availability

The code supporting the current study has not been deposited in a public repository but is available from the corresponding author on request. Variants were deposited in ClinVar[11] (accession numbers SCV001950995 - SCV001950998).

Acknowledgments

The authors are grateful to the families for their participation in this study. The authors also warmly thank Lucie Dos Santos for her contribution to the present work, Joanne Walker for the English language editing of the manuscript, as well as Pr Christel Thauvin-Robinet and Pr Laurence Faivre for their constructive and open discussions.

The Genotype-Tissue Expression (GTEx) Project was supported by the Common Fund of the Office of the Director of the National Institutes of Health, and by National Cancer Institute, National Human Genome Research Institute, National Heart, Lung and Blood Institute, National Institute on Drug Abuse, National Institute of Mental Health, National Institute of Neurological Disorders and Strokes. The data used for the analyses described in this manuscript were obtained from the GTEx Portal on 12/14/23.

Funding

No funding was obtained regarding this study.

Author Information

Conceptualization: M.T., E.C., S.K., G.F., A.L.; Data Curation: M.T., E.C.; Investigation: M.T., G.F., F.M., M.L., M.L.M., R.M.D., C.M., B.K., B.H., C.D.B., K.V.G., D.L., B.D., S.S., A.K.-C., R.A.J., M.W., B.C., A.D., M.Z.-M., A.G., C.B., P.V.B., F.B., G.L., P.M., C.F., B.G., V.P., A.V., D.B., A.L., S.K., E.C.; Supervision: E.C.; Writing-original draft: M.T., G.F., A.L., S.K., E.C.; Writing-review and editing: all the authors.

Ethics Declaration

Data were obtained in a diagnostic setting at individual centers after institutional review board (IRB) approval. The main IRB in this study is the IRB of the University Hospital of Angers, France. In addition, informed consent to publish clinical information was obtained from the parents of individuals reported in this article.

Conflict of Interest

The authors declare no conflicts of interest.

Additional Information

The online version of this article (https://doi.org/10.1016/j.gim.2024.101087) contains supplemental material, which is available to authorized users.

Affiliations

[1]Department of Medical Genetics, Angers University Hospital, Angers, France; [2]Mitovasc Unit, UMR CNRS 6015 INSERM 1083, University of Angers, Angers, France; [3]INSERM, Univ Brest, EFS, UMR 1078, GGB, Brest, France; [4]Univ Rouen Normandie, INSERM U1245 and Rouen University Hospital, Department of Pathology, Rouen, France; [5]Department of Genetics, Center for Rare Causes of Intellectual Disabilities and UPMC Research Group "Intellectual Disabilities and Autism" Paris, France; [6]Department of Genetics, La Pitié-Salpêtrière Hospital, Assistance Publique-Hôpitaux de Paris, Paris, France; [7]Sorbonne University, UPMC Univ Paris 06, UMR S 1127, INSERM U 1127, CNRS UMR 7225, ICM, Paris, France; [8]Department of Pediatric Neurology, Reference Center of Lysosomal Diseases, Trousseau Hospital, APHP, GRC ConCer-LD, Sorbonne Universities, UPMC University, Paris, France; [9]Department of Genetics, University Medical Center Utrecht, Utrecht, The Netherlands; [10]Department of Radiology, Angers University Hospital, Angers, France; [11]Heidelberg University, Medical Faculty of Heidelberg, Center for Child and Adolescent Medicine, Division of Pediatric Epileptology, Heidelberg, Germany; [12]Institute of Human Genetics, University of Leipzig Hospitals and Clinics, Leipzig, Germany; [13]Center for Medical Genetics, Department of Biomolecular Medicine, Gent, Belgium; [14]Department of Pathology, Angers University Hospital, Angers, France; [15]Department of Neuropediatrics, Angers University Hospital, Angers, France; [16]Department of Gynecology, Angers University Hospital, Angers, France; [17]Department of Pathology, Brest University Hospital, Brest, France; [18]UFR Des Sciences de Santé, INSERM-Université de Bourgogne UMR1231 GAD (Génétique des Anomalies du Développement), FHU-TRANSLAD, Dijon, France; [19]Unité Fonctionnelle Innovation en Diagnostic Génomique des Maladies Rares, FHU-TRANSLAD, CHU Dijon Bourgogne, Dijon, France

References

1. Long JE, Cobos I, Potter GB, Rubenstein JL. Dlx1&2 and Mash1 transcription factors control MGE and CGE patterning and differentiation through parallel and overlapping pathways. *Cereb Cortex*. 2009;19(suppl 1):i96-i106. http://doi.org/10.1093/cercor/bhp045
2. Lim L, Mi D, Llorca A, Marín O. Development and functional diversification of cortical interneurons. *Neuron*. 2018;100(2):294-313. http://doi.org/10.1016/j.neuron.2018.10.009
3. Kato M, Dobyns WB. X-linked lissencephaly with abnormal genitalia as a tangential migration disorder causing intractable epilepsy: proposal for a new term, "interneuronopathy". *J Child Neurol*. 2005;20(4):392-397. http://doi.org/10.1177/08830738050200042001
4. Katsarou AM, Moshé SL, Galanopoulou AS. Interneuronopathies and their role in early life epilepsies and neurodevelopmental disorders. *Epilepsia Open*. 2017;2(3):284-306. http://doi.org/10.1002/epi4.12062
5. Suske G, Bruford E, Philipsen S. Mammalian SP/KLF transcription factors: bring in the family. *Genomics*. 2005;85(5):551-556. http://doi.org/10.1016/j.ygeno.2005.01.005
6. Presnell JS, Schnitzler CE, Browne WE. KLF/SP transcription factor family evolution: expansion, diversification, and innovation in eukaryotes. *Genome Biol Evol*. 2015;7(8):2289-2309. http://doi.org/10.1093/gbe/evv141
7. Brayer KJ, Segal DJ. Keep your fingers off my DNA: protein-protein interactions mediated by C2H2 zinc finger domains. *Cell Biochem Biophys*. 2008;50(3):111-131. http://doi.org/10.1007/s12013-008-9008-5
8. Najafabadi HS, Mnaimneh S, Schmitges FW, et al. C2H2 zinc finger proteins greatly expand the human regulatory lexicon. *Nat Biotechnol*. 2015;33(5):555-562. http://doi.org/10.1038/nbt.3128
9. Liu Z, Zhang Z, Lindtner S, et al. Sp9 regulates medial ganglionic eminence-derived cortical interneuron development. *Cereb Cortex*. 2019;29(6):2653-2667. http://doi.org/10.1093/cercor/bhy133
10. Sobreira N, Schiettecatte F, Valle D, Hamosh A. GeneMatcher: a matching tool for connecting investigators with an interest in the same gene. *Hum Mutat*. 2015;36(10):928-930. http://doi.org/10.1002/humu.22844
11. Landrum MJ, Lee JM, Benson M, et al. ClinVar: improving access to variant interpretations and supporting evidence. *Nucleic Acids Res*. 2018;46(D1):D1062-D1067. http://doi.org/10.1093/nar/gkx1153
12. Autorité de Santé Haute. Protocole type d'examen autopsique fœtal ou néonatal - juin 2014 [Standard protocol for fetal or perinatal autopsy. Haute Autorité de santé]. *Ann Pathol*. 2014;34(6):415-433. http://doi.org/10.1016/j.annpat.2014.10.005
13. Guihard-Costa AM, Ménez F, Delezoide AL. Organ weights in human fetuses after formalin fixation: standards by gestational age and body weight. *Pediatr Dev Pathol*. 2002;5(6):559-578. http://doi.org/10.1007/s10024-002-0036-7
14. Feess-Higgins A, Larroche JC. *Development of the Human Foetal Brain, an Anatomical Atlas: Atlas Anatomique*. Inserm; 1987.
15. Miller JA, Ding SL, Sunkin SM, et al. Transcriptional landscape of the prenatal human brain. *Nature*. 2014;508(7495):199-206. http://doi.org/10.1038/nature13185
16. Radio FC, Pang K, Ciolfi A, et al. SPEN haploinsufficiency causes a neurodevelopmental disorder overlapping proximal 1p36 deletion syndrome with an episignature of X chromosomes in females. *Am J Hum Genet*. 2021;108(3):502-516. http://doi.org/10.1016/j.ajhg.2021.01.015
17. Karczewski KJ, Francioli LC, Tiao G, et al. The mutational constraint spectrum quantified from variation in 141,456 humans. *Nature*. 2020;581(7809):434-443. http://doi.org/10.1038/s41586-020-2308-7
18. Venselaar H, Te Beek TA, Kuipers RK, Hekkelman ML, Vriend G. Protein structure analysis of mutations causing inheritable diseases. An e-Science approach with life scientist friendly interfaces. *BMC Bioinformatics*. 2010;11:548. http://doi.org/10.1186/1471-2105-11-548
19. Kang HJ, Kawasawa YI, Cheng F, et al. Spatio-temporal transcriptome of the human brain. *Nature*. 2011;478(7370):483-489. http://doi.org/10.1038/nature10523
20. Polioudakis D, de la Torre-Ubieta L, Langerman J, et al. A single-cell transcriptomic atlas of human neocortical development during mid-gestation. *Neuron*. 2019;103(5):785-801.e8. http://doi.org/10.1016/j.neuron.2019.06.011
21. Lek M, Karczewski KJ, Minikel EV, et al. Analysis of protein-coding genetic variation in 60,706 humans. *Nature*. 2016;536(7616):285-291. http://doi.org/10.1038/nature19057
22. Bejerano G, Pheasant M, Makunin I, et al. Ultraconserved elements in the human genome. *Science*. 2004;304(5675):1321-1325. http://doi.org/10.1126/science.1098119
23. Klevit RE. Recognition of DNA by Cys2,His2 zinc fingers. *Science*. 1991;253(5026):1393. http://doi.org/10.1126/science.1896847
24. Zhang Q, Zhang Y, Wang C, et al. The zinc finger transcription factor Sp9 is required for the development of striatopallidal projection neurons. *Cell Rep*. 2016;16(5):1431-1444. http://doi.org/10.1016/j.celrep.2016.06.090
25. Zschocke J, Byers PH, Wilkie AOM. Mendelian inheritance revisited: dominance and recessiveness in medical genetics. *Nat Rev Genet*. 2023;24(7):442-463. http://doi.org/10.1038/s41576-023-00574-0

26. Shi Y, Wang M, Mi D, et al. Mouse and human share conserved transcriptional programs for interneuron development. *Science*. 2021;374(6573):eabj6641. http://doi.org/10.1126/science.abj6641
27. Ma T, Wang C, Wang L, et al. Subcortical origins of human and monkey neocortical interneurons. *Nat Neurosci*. 2013;16(11):1588-1597. http://doi.org/10.1038/nn.3536
28. Li J, Wang C, Zhang Z, et al. Transcription factors Sp8 and Sp9 coordinately regulate olfactory bulb interneuron development. *Cereb Cortex*. 2018;28(9):3278-3294. http://doi.org/10.1093/cercor/bhx199
29. Xu Z, Liang Q, Song X, et al. SP8 and SP9 coordinately promote D2-type medium spiny neuron production by activating Six3 expression. *Development*. 2018;145(14):dev165456. http://doi.org/10.1242/dev.165456
30. Tao G, Li Z, Wen Y, et al. Transcription factors *Sp8* and *Sp9* regulate medial ganglionic eminence-derived cortical interneuron migration. *Front Mol Neurosci*. 2019;12:75. http://doi.org/10.3389/fnmol.2019.00075
31. Wei S, Du H, Li Z, et al. Transcription factors Sp8 and Sp9 regulate the development of caudal ganglionic eminence-derived cortical interneurons. *J Comp Neurol*. 2019;527(17):2860-2874. http://doi.org/10.1002/cne.24712
32. Kawakami Y, Esteban CR, Matsui T, Rodríguez-León J, Kato S, Izpisúa Belmonte JC. Sp8 and Sp9, two closely related buttonhead-like transcription factors, regulate Fgf8 expression and limb outgrowth in vertebrate embryos. *Development*. 2004;131(19):4763-4774. http://doi.org/10.1242/dev.01331
33. Friocourt G, Parnavelas JG. Mutations in ARX result in several defects involving GABAergic neurons. *Front Cell Neurosci*. 2010;4:4. http://doi.org/10.3389/fncel.2010.00004
34. Ilsley MD, Huang S, Magor GW, Landsberg MJ, Gillinder KR, Perkins AC. Corrupted DNA-binding specificity and ectopic transcription underpin dominant neomorphic mutations in KLF/SP transcription factors. *BMC Genomics*. 2019;20(1):417. http://doi.org/10.1186/s12864-019-5805-z